



Dynamics of seawater carbonate chemistry, production, and calcification of a coral reef flat, central Great Barrier Reef

R. Albright¹, C. Langdon², and K. R. N. Anthony¹

¹Australian Institute of Marine Science, Townsville MC, Townsville, QLD 4810, Australia

²Rosenstiel School of Marine and Atmospheric Science, University of Miami, 4600 Rickenbacker Causeway, Miami, FL 33149, USA

Correspondence to: R. Albright (r.albright@aims.gov.au)

Received: 31 March 2013 – Published in Biogeosciences Discuss.: 3 May 2013

Revised: 28 August 2013 – Accepted: 16 September 2013 – Published: 28 October 2013

Abstract. Ocean acidification is projected to shift coral reefs from a state of net accretion to one of net dissolution this century. Presently, our ability to predict global-scale changes to coral reef calcification is limited by insufficient data relating seawater carbonate chemistry parameters to in situ rates of reef calcification. Here, we investigate diel and seasonal trends in carbonate chemistry of the Davies Reef flat in the central Great Barrier Reef and relate these trends to benthic carbon fluxes by quantifying net ecosystem calcification (nec) and net community production (ncp). Results show that seawater carbonate chemistry of the Davies Reef flat is highly variable over both diel and seasonal cycles. pH (total scale) ranged from 7.92 to 8.17, $p\text{CO}_2$ ranged from 272 to 542 μatm , and aragonite saturation state (Ω_{arag}) ranged from 2.9 to 4.1. Diel cycles in carbonate chemistry were primarily driven by ncp, and warming explained 35 % and 47 % of the seasonal shifts in $p\text{CO}_2$ and pH, respectively. Daytime ncp averaged $37 \pm 19 \text{ mmol C m}^{-2} \text{ h}^{-1}$ in summer and $33 \pm 13 \text{ mmol C m}^{-2} \text{ h}^{-1}$ in winter; nighttime ncp averaged -30 ± 25 and $-7 \pm 6 \text{ mmol C m}^{-2} \text{ h}^{-1}$ in summer and winter, respectively. Daytime nec averaged $11 \pm 4 \text{ mmol CaCO}_3 \text{ m}^{-2} \text{ h}^{-1}$ in summer and $8 \pm 3 \text{ mmol CaCO}_3 \text{ m}^{-2} \text{ h}^{-1}$ in winter, whereas nighttime nec averaged $2 \pm 4 \text{ mmol}$ and $-1 \pm 3 \text{ mmol CaCO}_3 \text{ m}^{-2} \text{ h}^{-1}$ in summer and winter, respectively. Net ecosystem calcification was highly sensitive to changes in Ω_{arag} for both seasons, indicating that relatively small shifts in Ω_{arag} may drive measurable shifts in calcification rates, and hence carbon budgets, of coral reefs throughout the year.

1 Introduction

Atmospheric carbon dioxide ($p\text{CO}_2$) has increased from approximately 280 to 390 ppm since the start of the industrial revolution due to anthropogenic activities such as the burning of fossil fuels, cement production, and land use changes (IPCC, 2007). Approximately 30 % of the carbon dioxide emitted each year into the atmosphere is absorbed by the world's surface oceans, causing a shift in the seawater carbonate chemistry (Canadell et al., 2007; Sabine et al., 2011). On entry into the ocean, CO_2 reacts with seawater via the following net chemical reaction:



As a result, concentrations of aqueous carbon dioxide, $[\text{CO}_2]_{\text{aq}}$, and bicarbonate, $[\text{HCO}_3^{-}]$, increase, while the concentration of carbonate, $[\text{CO}_3^{2-}]$, and the pH of seawater decrease (Broecker et al., 1979; Caldeira and Wickett, 2003; Sabine et al., 2004); this process is referred to as ocean acidification. Since preindustrial times, CO_2 uptake by the surface ocean waters has lowered seawater pH by approximately 0.1 units, which equates to an increase in acidity (i.e., the hydrogen ion concentration) of approximately 30 %. Carbonate ion concentrations in surface waters have simultaneously decreased by 11 % and 15 % in the tropics and Southern Ocean, respectively (Orr et al., 2005). Further reductions in pH of 0.3–0.5 units are projected by the end of this century as the oceans continue to absorb anthropogenic CO_2 (Sabine et al., 2004; IPCC, 2007).

A decrease in $[\text{CO}_3^{2-}]$ results in a decrease in the saturation state of calcium carbonate (CaCO_3), defined as

$$\Omega = [\text{Ca}^{2+}][\text{CO}_3^{2-}]/K'_{\text{sp}}, \quad (2)$$

where K'_{sp} is the solubility product for a particular mineral phase of CaCO_3 (e.g., aragonite, calcite). Aragonite is the dominant biogenic form of CaCO_3 secreted by many reef-building organisms, including corals. If $\Omega > 1$, seawater is supersaturated with respect to CaCO_3 , and conditions are favorable for CaCO_3 precipitation; conversely, if $\Omega < 1$, seawater is undersaturated with respect to CaCO_3 , and the dissolution of CaCO_3 is favored. The surface waters of the tropical oceans are currently supersaturated with respect to aragonite ($\Omega_{\text{arag}} = 4.0 \pm 0.2$, mean \pm SD); however, Ω_{arag} has steadily declined from a calculated 4.6 ± 0.2 one hundred years ago and is expected to continue declining to 3.1 ± 0.2 by the year 2065 and 2.8 ± 0.2 by 2100 (Kleypas et al., 1999).

Experimental results and models suggest that increases in atmospheric CO_2 and the associated declines in $[\text{CO}_3^{2-}]$ and Ω_{arag} of the ocean's surface waters will reduce rates of calcification on coral reefs (Gattuso et al., 1999; Langdon et al., 2000; Langdon and Atkinson, 2005; Anthony et al., 2008). Simultaneously, rates of bioerosion (Tribollet et al., 2009) and dissolution (Halley and Yates, 2000) are expected to increase. Because reef growth ultimately depends on the balance between constructive (e.g., CaCO_3 deposition) and destructive (e.g., bioerosion, dissolution, etc.) processes, there is concern that corals may be approaching a critical threshold, beyond which their ability to effectively form reefs will be compromised. Presently, our ability to predict global-scale changes to coral reef calcification is limited by insufficient data relating $p\text{CO}_2$, pH, $[\text{CO}_3^{2-}]$, and/or Ω to in situ rates of reef calcification.

Ocean acidification projections are based on trends from data collected in open ocean environments (Doney et al., 2009; Feely et al., 2009; Zeebe et al., 2012), and their implications for shallow, near-shore environments, such as coral reefs, are poorly understood. Coral reefs can naturally experience large fluctuations in seawater carbonate chemistry on both diurnal (Ohde and van Woerik, 1999; Shamberger et al., 2011; Shaw et al., 2012) and seasonal (Bates et al., 2010; Gray et al., 2012) timescales. The coral reef carbon cycle is mainly driven by two biological processes, organic carbon metabolism (photosynthesis and respiration) and inorganic carbon metabolism (calcification and dissolution). The extent to which these processes alter the carbonate chemistry of the overlying water column is a function of numerous environmental factors, including benthic community composition (Anthony et al., 2011), biological activity (which can vary with temperature, light and nutrient availability), physical forcing (e.g., temperature, salinity), tidal regime, water depth, and residence time (Falter et al., 2008, 2013). Accordingly, chemical conditions can vary from reef to reef and often differ from open ocean conditions. For example, Shaw et al. (2012) demonstrated that $p\text{CO}_2$ and pH values on the

Lady Elliot Island reef flat (Great Barrier Reef, Australia) can range from preindustrial values ($\sim 100 \mu\text{atm } p\text{CO}_2$ and pH 8.6) to future ocean acidification scenarios ($\sim 1300 \mu\text{atm } p\text{CO}_2$ and pH 7.6) over the course of a day. Understanding the significance of ocean acidification projections in the context of this background variability is imperative to gauging the susceptibility of reef ecosystems to projected changes in ocean chemistry.

Here, we investigate natural trends in carbonate chemistry of the Davies Reef flat (central Great Barrier Reef) on both diel and seasonal timescales, and we relate these trends to benthic carbon fluxes by quantifying net ecosystem calcification (nec) and net community production (ncp).

2 Methods

2.1 Study site

Davies Reef ($18^\circ 50' \text{S}$, $147^\circ 38' \text{E}$) is an open, lagoonal reef located in the mid-shelf of the central Great Barrier Reef, Australia (Fig. 1). The reef is located approximately 90–100 km northeast of Townsville, Queensland. Davies Reef is approximately 6 km long and 2.7 km wide; the reef flat faces the SE direction, and is approximately 300 m wide. The prevailing wind direction is from the southeast, and the tidal regime is semidiurnal. Current behavior on the reef flat is determined by the interaction of wind, tide and surface slope (Frith, 1983). Water flow across the reef flat is tidally dominated when the wind speed falls below $\sim 5 \text{ m s}^{-1}$. Tidal reversals occur such that reef flat currents flood from the lagoon to the reef crest and ebb from the crest to the lagoon (Frith, 1983). There is a wet season during summer from approximately November through April and a dry season during winter from approximately May through October.

2.2 Water sampling & analysis

2.2.1 Fixed stations

An automated water sampler (Fig. 2) was deployed on the protected (lagoonal) side of the reef flat (Fig. 1) to document diurnal variability in reef flat carbonate chemistry. The approximate average depth of the water sampler was $1.8 \pm 0.7 \text{ m}$ (mean \pm SD) but varied with tides (ranging from 0.5–3.5 m). The sampler was programmed to collect discrete water samples at 2 h intervals, by pumping reef water into pre-poisoned (0.05 % HgCl_2 by volume to inhibit biological activity; Dickson et al., 2007) 250 mL borosilicate bottles. Bottles were filled with reef water at a flow rate of $\sim 2 \text{ mL s}^{-1}$ ($\sim 2 \text{ min}$ per sample). The sampler was programmed to flush the lines for 30 s prior to filling a new sample bottle to avoid contamination of new samples with “old” water. Bottles were retrieved every 12 h and new, pre-poisoned bottles were deployed. The sampler was deployed

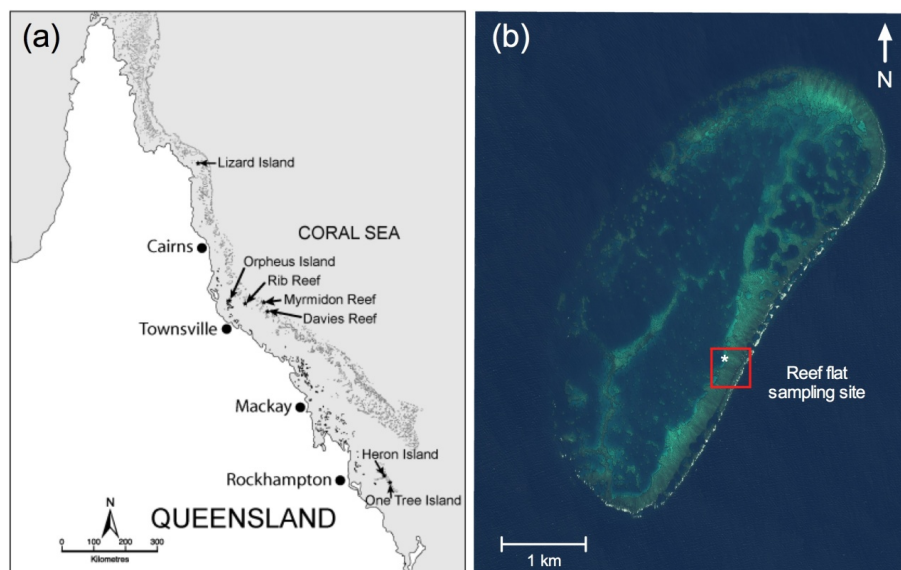


Fig. 1. (a) Map of Queensland, Australia, showing the location of Davies Reef within the central Great Barrier Reef (www.imos.org). (b) Quickbird image of Davies Reef ($18^{\circ}50' S$, $147^{\circ}38' E$) with the reef flat study area denoted by a red square. The asterisk denotes the location of the automated water sampler. Lagrangian transects were conducted within the 300 m^2 sampling box.

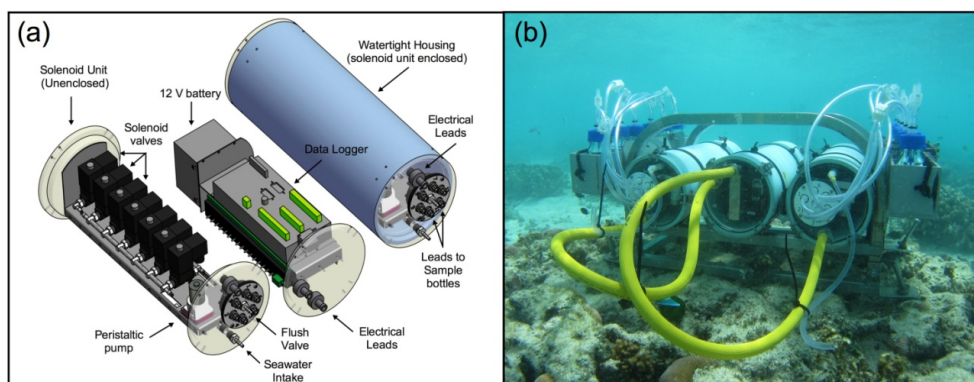


Fig. 2. Automated water sampler that was deployed at the lagoonal edge of the reef flat for 10 days in austral summer (17–27 January 2012) and 9 days in winter (29 July–6 August 2012). The sampler collected discrete water samples at 2 h intervals during the course of each deployment for the analysis of total alkalinity (A_T) and dissolved inorganic carbon (C_T). (a) Schematic of water sampler design. (b) Sampler deployed on the reef flat.

during the period 17–27 January 2012 in austral summer and 29 July–6 August 2012 in austral winter.

2.2.2 Transects

net and ncp of the Davies reef flat were measured using a Lagrangian approach. This method involves measuring total alkalinity (A_T) and dissolved inorganic carbon (C_T) immediately before a parcel of water traverses the reef flat and immediately downstream of the reef community. The changes in A_T and C_T were corrected for transit time and water depth profile to produce a net rate at which the community altered the chemistry of the overlying water column (Eqs. 1, 2). A representative transect, with corresponding decreases in A_T

and C_T , is shown in Fig. S1 of the Supplement. This method is limited to environments that experience unidirectional flow of water, and it has been widely applied to reef flats that experience unidirectional flow during incoming/outgoing tides or due to waves breaking across a reef crest (Langdon et al., 2010). At the Davies Reef study site, biological zones are broad and perpendicular to the direction of water flow; lateral mixing was, therefore, considered an insignificant source of error (Langdon et al., 2010).

Lagrangian transport was measured by following water parcels using a small boat and a hand-held GPS (2–5 m precision) to record the location of the parcel as it traversed the reef flat. Water parcels were identified using fluorescein

dye during the day and drifters (60 cm tall and 75 cm wide) at night. In a pilot study, the behaviors of the drogue and dye were compared by employing both methods simultaneously ($n = 11$). Results indicate that at higher wind speeds, the drifter speeds exceed the dye speeds (Fig. S2 of the Supplement). In our study, drogues were only employed during night transects, which were conducted at an average wind speed of $5.6 \pm 0.9 \text{ m s}^{-1}$ (mean \pm SD), ranging from $4.0\text{--}7.2 \text{ m s}^{-1}$. At the average wind speed of 5.6 m s^{-1} , we estimate that the drifter overestimated the current speed by less than 4%. One transect was conducted at 7.2 m s^{-1} , for which the current speed would have been overestimated by approximately 14%. For this transect, the transit time of the drogue was corrected to obtain a speed which would more closely approximate the dye (according to the relationship defined in Fig. S2). Falter et al. (2008) reported that dye patch speeds were highly correlated with depth-averaged current speeds calculated from ADCP data. Thus, drogue speed in our study was corrected to the dye speed as opposed to the other way around.

Discrete water samples were taken in duplicate at the beginning and end of each Lagrangian transect. Samples were taken in 250 mL borosilicate bottles filled at the water's surface and immediately poisoned with 125 μL HgCl_2 (0.05 % by volume) to inhibit biological activity. Water depth was measured using a hand-held depth sounder alongside of the dye patch/drifter at regular intervals along each transect and averaged. Transects were repeated 48 times over the course of 14 days in 2 seasons to develop composite diel curves for calcification and production.

2.2.3 Carbonate chemistry

Water samples were transported to the Australian Institute of Marine Science (AIMS) where they were analyzed for total alkalinity (A_T) and dissolved inorganic carbon (C_T) using a VINDTA 3C[®] (Versatile Instrument for the Determination of Total dissolved inorganic carbon and Alkalinity; Marianda, Kiel, Germany) and a UIC CO₂ coulometer detector (UIC Inc., Joliet, USA). Accuracy was checked against certified seawater reference material (from A. Dickson, Scripps Institute of Oceanography, Batch 106). $p\text{CO}_2$, pH_T (total scale), and aragonite saturation state (Ω_{arag}) were calculated as a function of the measured salinity, temperature, A_T , and C_T using the program CO2SYS (from E. Lewis, Brookhaven National Laboratory/Lewis and Wallace, 1998); dissociation constants for carbonate and boric acid were determined by Mehrbach et al. (1973) as refit by Dickson and Millero (1987), and the dissociation constant for boric acid was determined by Dickson (1990).

2.2.4 Physical conditions

Temperature, light (PAR at 0.8 m depth), and wind data were obtained from the AIMS Weather Station at Davies Reef (<http://data.aims.gov.au/aimsrtlds/station.xhtml?station=4>), and salinity data were obtained from the Integrated Marine Observing System (IMOS 2012). The Davies Reef weather tower is located ~ 1.5 km from the center of the reef flat site, in the Davies Reef lagoon.

2.3 Calculations

Changes in seawater carbon chemistry between upstream and downstream sampling points can be used to calculate rates of nec and ncp. In most coral reef systems, changes in total alkalinity (A_T) are caused primarily by calcification and dissolution of CaCO_3 whereby two moles of A_T are consumed (produced) for every mole of CaCO_3 produced (dissolved). Accordingly, nec ($\text{mmol CaCO}_3 \text{ m}^{-2} \text{ h}^{-1}$) can be calculated as

$$\text{nec} = -0.5\rho h \frac{\Delta A_T}{\Delta t}, \quad (3)$$

where ΔA_T is the change in total alkalinity between the upstream and downstream locations (mmol kg^{-1}), ρ is the seawater density (kg m^{-3}), h is the water depth (m), and Δt is the duration of the transect (h).

C_T is affected by calcification, dissolution, photosynthesis, and respiration. ncp ($\text{mmol C m}^{-2} \text{ h}^{-1}$) can be calculated using changes in C_T after taking into account nec and gas exchange:

$$\text{ncp} = -h\rho \frac{(\Delta C_T - 0.5\Delta A_T)}{\Delta t} - kS(p\text{CO}_2w - p\text{CO}_2a), \quad (4)$$

where ΔC_T is the change in dissolved inorganic carbon between the upstream and downstream locations (mmol kg^{-1}), and the term $kS(p\text{CO}_2w - p\text{CO}_2a)$ approximates gas exchange where k is the gas transfer velocity, S is the solubility of CO_2 calculated as a function of salinity and temperature, and $(p\text{CO}_2w - p\text{CO}_2a)$ is the difference in $p\text{CO}_2$ between the surface ocean and the atmosphere. All other parameters are defined as above. The wind speed parameterization of Ho et al. (2006) was used to calculate k , which ranged from 5.8 to 16.7 cm h^{-1} , with a mean of 10.3 cm h^{-1} . Atmospheric $p\text{CO}_2$ was assumed to be 394 ppm. Resulting gas exchange estimates were small in comparison to ncp, ranging from -0.11 to $0.13 \text{ mmol C m}^{-2} \text{ h}^{-1}$. Because gas exchange averaged 0.32 % of ncp (ranging from 0 % to 1.9 %), this term was treated as negligible, simplifying the equation to the following:

$$\text{ncp} = -h\rho \frac{(\Delta C_T - 0.5\Delta A_T)}{\Delta t}, \quad (5)$$

Pearson's correlations were computed to assess the relationship between nec and aragonite saturation state (Ω_{arag}). The relationship between A_T and C_T was evaluated by conducting Model II (Major Axis, MA) regressions in R.

2.4 Light response curves

Productivity- and calcification-irradiance curves were fitted to data using linear or non-linear curve fitting (Gattuso et al., 1996) (Graphpad Prism 5.0 for Mac OS X). The hyperbolic tangent function $y = a \cdot \tanh(-x/b) + c$ produced the best fit for the productivity-irradiance curve, and the calcification-irradiance curve was modeled using a linear function.

2.5 Benthic community structure

Benthic surveys were conducted in both summer and winter to characterize the underlying community structure of the reef flat site. Five, 200 m transects were laid on the reef flat perpendicular to the reef front, spaced 50 m apart. Photographs were taken of 0.5 m² quadrats at 5 m intervals (40 photos per transect). Photos were analyzed using Coral Point Count software with Excel extensions (CPCe) using 20 random points per quadrat. The benthos was assigned to one of five main categories: (1) live coral; (2) algae (including macroalgae, turf, and cyanobacteria); (3) coralline algae (CCA); (4) CaCO₃ substrate including sand, CaCO₃ rock (e.g., old, dead coral), and/or rubble (i.e., substrate with the potential to undergo dissolution); (5) and “other”, including sponges, gorgonians, zoanthids, giant clams, etc. Where morphologic forms of CaCO₃ (e.g., rubble, CaCO₃ rock) were covered with biologically active groups (e.g., turf, coralline algae, cyanobacteria), the biologically active group was scored.

3 Results

3.1 Physical conditions

3.1.1 Summer

Noontime irradiance, as measured at 0.8 m depth, ranged from 563 to 1240 $\mu\text{mol m}^{-2} \text{s}^{-1}$, averaging $1099 \pm 186 \mu\text{mol m}^{-2} \text{s}^{-1}$. Winds were predominantly from the east/southeast and averaged $6 \pm 2 \text{ m s}^{-1}$ (mean \pm SD), ranging from 2 to 12 m s^{-1} . The tidal height ranged from 0.5 to 3.5 m. Average temperature was $28.5 \pm 0.2 \text{ }^\circ\text{C}$ (ranging from 28.1 to 28.9 $^\circ\text{C}$) and salinity was 35.0 ± 0.1 .

3.1.2 Winter

Noontime irradiance ranged from 772 to 1023 $\mu\text{mol m}^{-2} \text{s}^{-1}$, averaging $908 \pm 99 \mu\text{mol m}^{-2} \text{s}^{-1}$. Winds were predominantly from the east/southeast and averaged $6 \pm 2 \text{ m s}^{-1}$ (mean \pm SD), ranging from 2–10 m s^{-1} . The tidal height ranged from 0.5 to 3.4 m. Average temperature was $22.4 \pm 0.1 \text{ }^\circ\text{C}$ (ranging from 22.1 to 22.7 $^\circ\text{C}$) and salinity was 35.6 ± 0.1 .

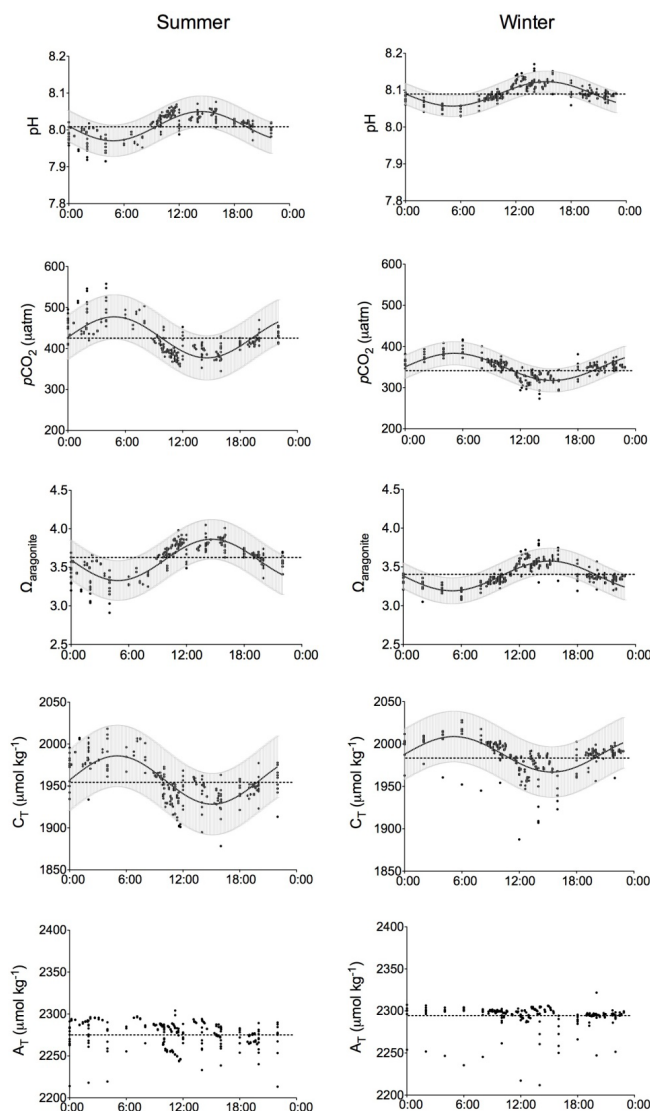


Fig. 3. Composite diel curves of carbonate chemistry parameters by season for the Davies Reef flat. Data points show reef flat data from 10 and 9 consecutive days in January and August, respectively. Solid black lines represent best-fit curves, and shaded areas represent 95 % confidence intervals for future data points. Dashed horizontal lines represent average daily conditions.

3.2 Diel patterns in seawater carbonate chemistry

C_T and $p\text{CO}_2$ were highest just before dawn, following a steady increase throughout the night and lowest just before dusk following a steady decrease during the day (Fig. 3). Diel patterns in pH_T and aragonite saturation state (Ω_{arag}) mirrored those for C_T and $p\text{CO}_2$ but with highs at dusk and lows at dawn. Tides resulted in small diel changes in temperature and salinity of approximately 1 $^\circ\text{C}$ and < 0.1 units, respectively. All measured and calculated physical and chemical parameters are presented in Table 1.

Table 1. Seasonal averages (mean \pm SD) and ranges of measured* and calculated physical and chemical parameters.

	T^* °C	S^*	A_T^* $\mu\text{mol kg}^{-1}$	C_T^* $\mu\text{mol kg}^{-1}$	pH_T	$p\text{CO}_2$ μatm	Ω_{arag}	CO_3^{2-} $\mu\text{mol kg}^{-1}$	n
Summer									
Mean \pm 1 SD	28.5 \pm 0.2	35.0 \pm 0.1	2276 \pm 16	1954 \pm 25	8.03 \pm 0.03	404 \pm 40	3.7 \pm 0.2	228 \pm 13	227
Range	28.1–28.9	34.9–35.1	2213–2304	1878–2018	7.92–8.10	325–542	2.9–4.1	181–253	
Winter									
Mean \pm 1 SD	22.3 \pm 0.1	35.6 \pm 0.1	2294 \pm 13	1985 \pm 19	8.09 \pm 0.02	348 \pm 24	3.4 \pm 0.1	217 \pm 9	211
Range	22.1–22.7	35.5–35.7	2212–2322	1887–2028	8.03–8.17	275–420	3.0–3.8	195–245	

Table 2. Length, depth, velocity, and sample size (n) of Lagrangian transects by season.

	Length m	Depth m	Velocity cm s^{-1}	n , daytime (sample times)	n , nighttime (sample times)
Summer					
Mean \pm 1 SD	210 \pm 59	1.7 \pm 0.5	11.6 \pm 5.7	10 (09:30–16:00)	7 (19:00–07:00)
Range	85–316	1.1–2.8	4.2–22.5	–	–
Winter					
Mean \pm 1 SD	193 \pm 55	1.9 \pm 0.4	10.1 \pm 3.8	20 (09:00–15:30)	11 (19:00–23:00)
Range	77–397	1.2–2.6	3.1–17.5	–	–

3.3 Carbon fluxes

A total of 48 nec and ncp rates were calculated over both seasons. Details of Lagrangian transects are given in Table 2.

3.3.1 Summer

nec ranged from 5 to 17 $\text{mmol CaCO}_3 \text{ m}^{-2} \text{ h}^{-1}$ during the day, averaging $11 \pm 4 \text{ mmol CaCO}_3 \text{ m}^{-2} \text{ h}^{-1}$ (mean \pm SD). At night, nec ranged from -3 to $7 \text{ mmol CaCO}_3 \text{ m}^{-2} \text{ h}^{-1}$, averaging $2 \pm 4 \text{ mmol CaCO}_3 \text{ m}^{-2} \text{ h}^{-1}$. There was a positive correlation between nec and Ω_{arag} , Pearson $r = 0.51$, $n = 17$, and $p = 0.034$. Using local times for sunrise (06:00) and sunset (19:00), a day length of 13 h was used to estimate an average net daily calcification rate of $6.9 \pm 5.6 \text{ mmol CaCO}_3 \text{ m}^{-2} \text{ h}^{-1}$ (mean \pm SD).

ncp ranged from 9 to $64 \text{ mmol C m}^{-2} \text{ h}^{-1}$ during the day, averaging $37 \pm 19 \text{ mmol C m}^{-2} \text{ h}^{-1}$ (mean \pm SD). At night, ncp ranged from -65 to $1 \text{ mmol C m}^{-2} \text{ h}^{-1}$, averaging $-30 \pm 25 \text{ mmol C m}^{-2} \text{ h}^{-1}$ (i.e., net respiration).

3.3.2 Winter

nec ranged from 2 to $14 \text{ mmol CaCO}_3 \text{ m}^{-2} \text{ h}^{-1}$ during the day, averaging $8 \pm 3 \text{ mmol CaCO}_3 \text{ m}^{-2} \text{ h}^{-1}$ (mean \pm SD). At night, nec ranged from -4 to $4 \text{ mmol CaCO}_3 \text{ m}^{-2} \text{ h}^{-1}$, averaging $-1 \pm 3 \text{ mmol CaCO}_3 \text{ m}^{-2} \text{ h}^{-1}$ (i.e., net dissolution). There was a positive correlation between nec and Ω_{arag} , Pearson $r = 0.49$, $n = 31$, and $p = 0.005$. Using local times for sunrise (06:40) and sunset (18:00), a day length of 11.33 h was used to estimate an average net daily calcification rate of

$3.2 \pm 4.2 \text{ mmol CaCO}_3 \text{ m}^{-2} \text{ h}^{-1}$, approximately half that of the summer rate.

ncp ranged from 1 to $52 \text{ mmol C m}^{-2} \text{ h}^{-1}$ during the day, averaging $33 \pm 13 \text{ mmol C m}^{-2} \text{ h}^{-1}$ (mean \pm SD). At night, ncp ranged from -14 to $5 \text{ mmol C m}^{-2} \text{ h}^{-1}$, averaging $-7 \pm 6 \text{ mmol C m}^{-2} \text{ h}^{-1}$ (i.e., net respiration).

3.4 Light response curves

Best fits for productivity- and calcification-irradiance curves are presented in Fig. 5.

3.5 Benthic surveys

The benthos at the study site was dominated by algae (56–58 %, including macroalgae, turf, and cyanobacteria) with live coral (8–10 %) and crustose coralline algae (8–9 %) each representing minor groups (Table 3). Approximately 22–24 % of the benthic habitat consisted of exposed CaCO_3 substrate. The relative abundance of the benthic groups remained relatively stable between summer and winter during the study period.

4 Discussion

4.1 Trends in carbonate chemistry

Seawater carbonate chemistry observed at the Davies Reef flat was highly variable over both diel and seasonal timescales. pH_T ranged from 7.92 to 8.17, $p\text{CO}_2$ ranged from 272 to 542 μatm , and Ω_{arag} ranged from 2.9 to 4.1.

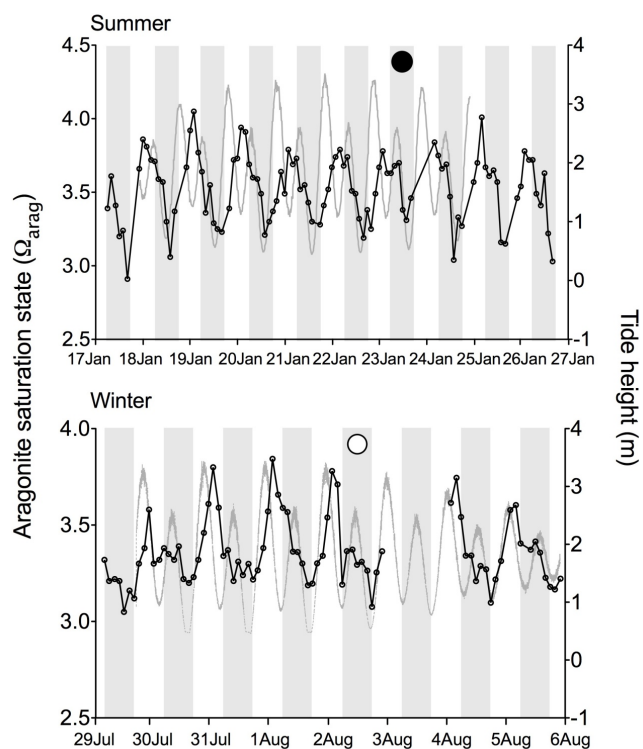


Fig. 4. Daily times series of aragonite saturation state (Ω_{arag}) of the Davies Reef flat in summer (January) and winter (August) 2012. Data were collected using an automated water sampler that was deployed at the lagoonal edge of the reef flat. Light and dark cycles are denoted by shading, and moon phases are indicated by open (full moon) and closed (new moon) circles. Tide height is indicated by the grey line. Gaps in the data correspond to when the instrument was removed from the reef for maintenance.

Table 3. Percent cover (mean \pm 1 SD) of major benthic groups on the Davies Reef flat by season. Benthos was assigned to one of five categories: (1) live coral; (2) algae, including macroalgae, turf, and cyanobacteria; (3) coralline algae; (4) CaCO_3 substrate, including sand, CaCO_3 rock (e.g., old, dead coral), and/or rubble (i.e., substrate with the potential to undergo dissolution); and (5) “other”, including sponges, gorgonians, zoanthids, etc. When morphologic forms of CaCO_3 (e.g., rubble, CaCO_3 rock) were covered with biologically active groups (e.g., turf, coralline algae, cyanobacteria), the biologically active group was scored.

	Live coral	Algae	Coralline algae	CaCO_3 substrate	“Other”
Summer	10 \pm 2	58 \pm 3	8 \pm 4	22 \pm 5	< 2
Winter	8 \pm 2	56 \pm 3	9 \pm 3	24 \pm 3	< 3

These ranges are consistent with those reported for other studies of extensive shallow-water reef flat systems (Shaw et al., 2012, Table 3). Diel cycles of $p\text{CO}_2$ and Ω_{arag} are largely driven by rates of primary production (Anthony et al., 2011; Kleypas et al., 2011; Shamberger et al., 2011; Shaw et

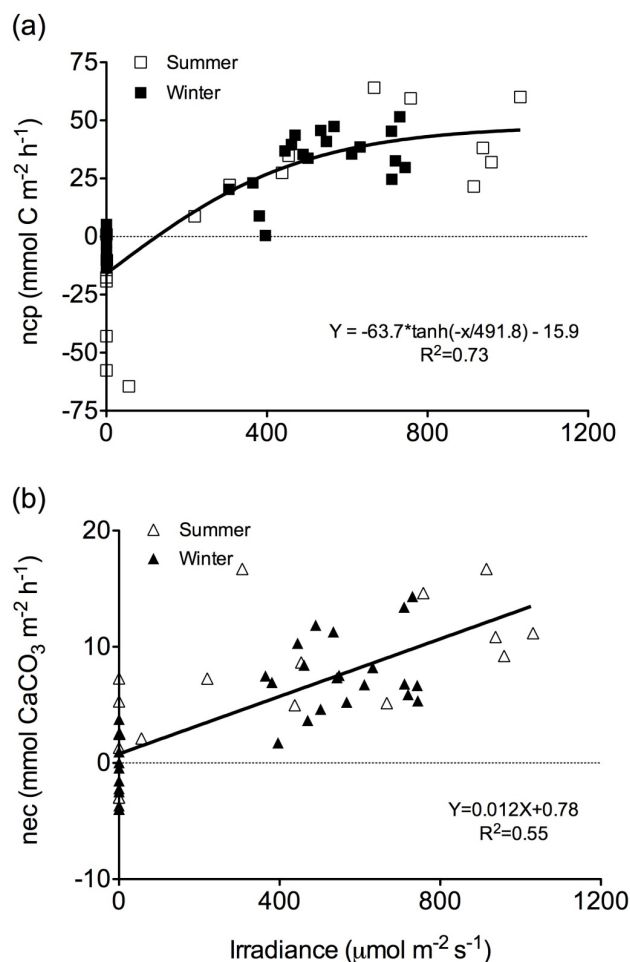


Fig. 5. (a) Productivity-irradiance and (b) calcification-irradiance curves for the Davies Reef flat community (combined seasons).

al., 2011) such that photosynthetic uptake of CO_2 during the day results in an elevated saturation state when calcification is at its highest. While the light–dark cycle fundamentally controls the phase of the diel carbonate cycle via primary production, the amplitude of the cycle is influenced by a variety of factors including benthic community composition, tidal regimes, water depth, and residence time. The effects of tides on the amplitude of diel cycling is highly visible in winter (Fig. 4). The larger of the two mixed diurnal tides resulted in greater changes in Ω_{arag} , while the smaller diurnal tide resulted in a dampened signal.

Seasonal variability in pH_T , $p\text{CO}_2$, and Ω_{arag} is the result of both physical processes (e.g., temperature forcing) and biological processes driving variation in nec and ncp. Temperature effects were examined using sensitivity analyses whereby in situ pH_T , $p\text{CO}_2$, temperature, and salinity were used as input parameters to the program CO_2SYS (Lewis and Wallace, 1998), and pH_T and $p\text{CO}_2$ were recorded as outputs at the mean seasonal temperature (see Gray et al., 2012). Temperature-adjusted data indicate that 0.03 units of the 0.06

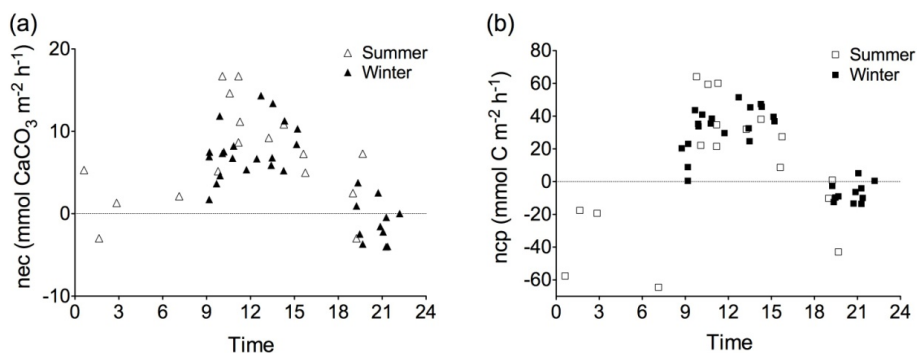


Fig. 6. (a) Net ecosystem calcification (nec) and (b) net community production (ncp) of the Davies Reef flat by time of day.

pH_T unit seasonal change (47 %) (Table 1) and 19 μ atm of the 56 μ atm seasonal p CO₂ change (35 %) were due to cooling from 28.5 °C in summer to 22.3 °C in winter.

4.2 Diel and seasonal variation in biological activity

In general, nec and ncp increased throughout the day and decreased into the evening. Metabolic rates were strongly coupled to incident light levels (Fig. 5), but were highly variable by time of day (Fig. 6). This variability is likely due to lower sampling resolution for the Lagrangian transects compared to the autosampler measurements, fluctuations in light levels, flow, and slightly different trajectories between runs, thereby tracking over benthic communities with slightly different compositions. Another source of variation is the ocean source water; Davies Reef experiences tidal reversals such that transects run from crest to lagoon during outgoing tides and from lagoon to crest during incoming times. Sensitivity analyses indicated that transect length was not a significant source of variation in rate data. Variable rates of nec at the same time of day on subsequent days can be observed in other, similar studies. For example, Silverman et al. (2012) report values for nec that range from ~ 6 to 18 mmol m⁻² h⁻¹ at $\sim 09:30$ and from 7 to 20 mmol m⁻² h⁻¹ at $\sim 12:00$.

The reef flat generally showed positive nec during the day and negative nec at night. Daytime nec and ncp were slightly higher in summer than in winter, a finding that is consistent with numerous previous studies (e.g., Shamberger et al., 2011; Table 2). Net calcification continued at low rates at night in summer, but net dissolution occurred at low rates at night in winter. While we did not observe values of Ω_{arag} lower than 2.9, dissolution occurred at night in waters that remained supersaturated with respect to calcium carbonate. Dissolution in supersaturated waters has been reported previously in other reef systems (Yates and Halley, 2006) and is believed to be the result of undersaturation in pore waters, bioerosion of sediments by endolithic microbes and boring forams, and/or dissolution of more soluble forms of calcium carbonate (e.g., high-Mg calcite) (Yates and Halley, 2006; Santos et al., 2012).

Average nighttime respiration in summer (-30 ± 25 mmol C m⁻² h⁻¹, mean \pm SD) was approximately fourfold higher than in winter (-7 ± 6 mmol C m⁻² h⁻¹). This difference was primarily driven by three night transects in summer that yielded anomalously high respiration rates (> 40 mmol C m⁻² h⁻¹; Fig. 6b). While these rates are high in comparison to the other nighttime data from this study, comparable rates of nighttime respiration have been reported for the Kaneohe Bay barrier reef (Shamberger et al., 2011), and we have little reason to believe that these transects are unrepresentative. By omitting the anomalous transects, summer nighttime respiration ranged from -19 to 1 mmol C m⁻² h⁻¹, averaging -12 ± 9 mmol C m⁻² h⁻¹.

Using local times for sunrise and sunset, the daily average nec was estimated to be 6.9 ± 5.6 mmol CaCO₃ m⁻² h⁻¹ (mean \pm SD) in summer and 3.2 ± 4.2 mmol CaCO₃ m⁻² h⁻¹ in winter. When scaled up, these values yield a daily average NEC of 166 mmol (16.6 g) CaCO₃ m⁻² d⁻¹ in summer and 77 mmol (7.7 g) CaCO₃ m⁻² d⁻¹ in winter and an annual calcification rate of 4.4 kg CaCO₃ m⁻² yr⁻¹ (assuming 0.5 yr or 182.5 days at each net rate). This annual calcification rate is consistent with the average calcification rate of 4 ± 0.7 kg m⁻² CaCO₃ yr⁻¹ reported to occur widely in Indo-Pacific coral reef flat environments (Kinsey, 1985). The average summer daytime net calcification in this study, 11 ± 4 mmol CaCO₃ m⁻² h⁻¹ (mean \pm SD), is comparable to values reported for GBR sites with comparable coral cover during similar times of year; Silverman et al. (2012) reported average summer daytime net calcification for the One Tree Island reef flat (13.7 % coral cover) as 11 ± 7 mmol CaCO₃ m⁻² h⁻¹.

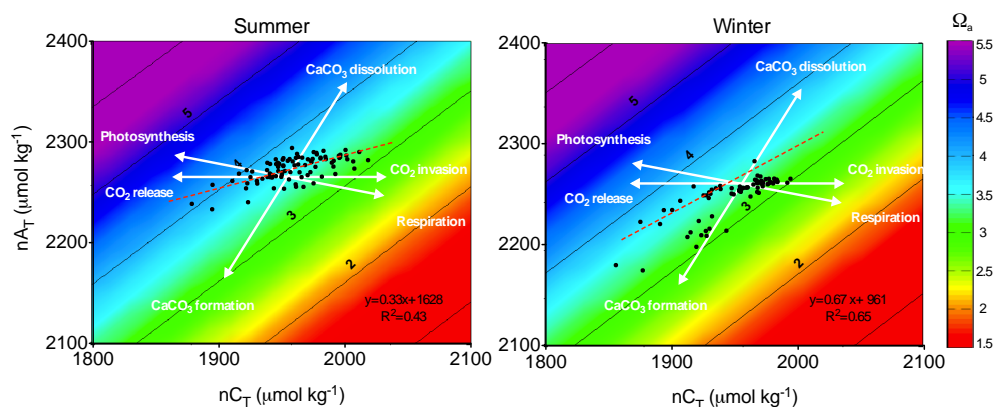


Fig. 7. Total alkalinity versus dissolved inorganic carbon diagrams by season. Vectors illustrate the direction of the effects of photosynthesis, respiration, calcification, and dissolution on A_T , C_T , and Ω_{arag} . Omega isopleths correspond to 28.3 °C in summer and 22.5 °C in winter. A_T and C_T data were normalized to a salinity of 35 (nA_T and nC_T , respectively) by multiplying A_T and C_T data by the ratio of 35 to the measured in situ salinity. Data points show reef flat data collected from the water sampler time series. The slope of the A_T – C_T relationship is less than the slope of the omega isopleths, indicating that biological activity during the day elevates the saturation state of the overlying water column, benefiting calcification and partially offsetting the effects of ocean acidification. See text for details.

4.3 Historical comparisons

Assessing historical trends in reef community metabolism is often complicated by a lack of baseline data, including data on changes in benthic community composition. Nonetheless, at least two recent studies conducted on the Great Barrier Reef address long-term trends in carbon cycling on coral reefs. Carbon turnover rates of the One Tree Island reef were originally studied in the 1970s and 1980s (Kinsey, 1978, 1979) and more recently by Silverman et al. (2012). Silverman et al. (2012) report drastic reductions in net calcification (~44%) that are primarily attributed to a threefold increase in nighttime dissolution rates. In contrast, Shamberger et al. (2011) report rates of net ecosystem calcification for reefs in Kaneohe Bay that are comparable to values reported from the 1970s. These findings were surprising given that $p\text{CO}_2$ was substantially lower and Ω_{arag} was higher in the 1970s (Kinsey, 1985).

The results of this study are partly consistent with the results of Barnes (1983, 1988) whereby seasonality in community productivity and calcification were evaluated by floating an instrument package carrying pH and oxygen electrodes across the Davies Reef flat. Barnes reported seasonal variations in productivity and calcification of the Davies Reef flat, with net productivity averaging 45% higher, and net calcification averaging 30–40% higher in summer than in winter (Barnes, 1988). Daily net calcification rates of the reef flat were 16 g $\text{CaCO}_3 \text{ m}^{-2} \text{ d}^{-1}$ in summer (1981) and 11.9 g $\text{CaCO}_3 \text{ m}^{-2} \text{ d}^{-1}$ in winter (1984), compared to 16.6 (summer) and 7.7 (winter) g $\text{CaCO}_3 \text{ m}^{-2} \text{ d}^{-1}$ in the present study. Barnes also reported higher rates of respiration in summer, an observation that is consistent with the present study. Barnes attributed the seasonality in community productivity to seasonal shifts in community composi-

tion, whereby epilithic algal blooms occurred in summer and died in winter. Seasonal shifts in algal biomass (or other benthic community groups) were not observed in the present study. The seasonal differences in community metabolism measured here are likely due to the warmer temperatures in summer driving higher rates of calcification and productivity. Other contributing factors may have been light and/or nutrients; in the present study, average noontime irradiance was slightly higher in summer (1099 $\mu\text{mol m}^{-2} \text{ s}^{-1}$) than winter (908 $\mu\text{mol m}^{-2} \text{ s}^{-1}$). Nutrient levels were not measured and cannot be excluded as a source of seasonal differences; however, Kinsey (1978) showed that changes in salinity and nutrients had a negligible effect on changes in alkalinity in coral reefs. In Barnes' study, both light and temperature were elevated in summer and may have also been a contributing factor to the seasonal differences that were reported; however, the influence of these factors on seasonal differences was not addressed.

Differences in methodology and technology preclude a robust assessment of changes in reef metabolism over time. However, these studies indicate that while some reefs (One Tree Island) may have experienced drastic changes in net calcification over time, others, including Kaneohe Bay and Davies Reef, may have been less heavily affected.

4.4 Implications of the A_T – C_T relationship

We further analyzed the A_T – C_T relationship to explore to what extent benthic carbon fluxes alter the aragonite saturation state of the overlying water (Fig. 7). Here, vectors indicate the theoretical effects of photosynthesis–respiration and calcification–dissolution on A_T and C_T : for every mol of organic carbon produced (via photosynthesis), one mol of C_T is consumed, and A_T remains unchanged; for every mol of

CaCO₃ produced (calcification), A_T decreases by 2 mol and C_T decreases by 1 mol. Because photosynthesis–respiration (ncp) and calcification–dissolution (nec) affect A_T and C_T differently, the slope of the A_T – C_T relationship indicates the balance between these two processes (i.e., the nec : ncp ratio). The nec : ncp ratio is given by $\frac{1}{(2/m)-1}$, where m is the slope of the A_T – C_T line. The slope of the omega isopleths in Fig. 7 is approximately 0.93 in A_T – C_T space, which corresponds to a nec : ncp ratio of 0.87. Generally, if the slope of the A_T – C_T relationship approximates the slope of the omega isopleths, biological activity shifts points along a given isopleth and does not alter the saturation state of the overlying water column. Alternatively, if the A_T – C_T relationship crosses the isopleths (i.e., the slope of the A_T – C_T relationship is less than the slope of the isopleths), biological activity will increase the saturation state during the day and decrease the saturation state during the night. Using the time series data collected from the water sampler station, the slopes of the A_T – C_T relationships for Davies Reef are 0.33 and 0.67 for summer and winter, respectively; these slopes correspond to nec : ncp ratios of 0.20 for summer and 0.50 for winter, indicating that daytime biological activity increases the saturation state of the water with time. The slope of the A_T – C_T relationship may prove a valuable indicator of reef function because it reflects the balance between calcification and production, providing information concerning benthic carbon fluxes and biogeochemical cycling; phase shifts (e.g., from coral-dominated to algal-dominated systems) and/or significant stress events (e.g., bleaching) would be expected to be reflected in this slope, possibly rendering it a useful parameter for broad-scale reef monitoring programs. If comparisons of A_T – C_T plots are made over time, care should be taken to minimize sources of variation, including analytical differences between measurements sets, sampling times, etc.

4.5 Relationship between calcification and saturation state

Net ecosystem calcification was positively correlated with Ω_{arag} for both seasons. For logistical reasons (inability to access the reef flat at extreme low tides), we were restricted to working on the reef flat in water depths of ≥ 1 m. Consequently, rate data were collected over a relatively narrow range of Ω_{arag} values in comparison to other studies (e.g., Shamberger et al., 2011; Shaw et al., 2012; Falter et al., 2012; Silverman et al., 2007; Yates and Halley, 2006). In summer, the range of saturation states during which Lagrangian transects were conducted was 3.42–3.94 (0.52 units), and in winter it was 3.29–3.69 (0.4 units). The relatively narrow range of Ω_{arag} values for which we were able to collect rate data precludes a robust analysis of the relationship between Ω_{arag} and nec (e.g., the identification of ‘threshold’ values for Ω_{arag} at which point the reef shifts from a state of net accretion to net dissolution). However, the significant correlation between nec and Ω_{arag} over a narrow range of Ω_{arag} values

suggests that relatively small declines in Ω_{arag} resulting from ocean acidification may drive measurable declines in community calcification in reef habitats.

Supplementary material related to this article is available online at <http://www.biogeosciences.net/10/6747/2013/bg-10-6747-2013-supplement.zip>.

Acknowledgements. The authors are grateful to D. Kinsey for discussion that greatly improved the design of this study. We are indebted to E. Clarkin, B. Mason, C. Huete-Stauffner, N. Cantin, P. Kaniewska, E. Matson, N. Jeeves and the staff of the RV *Cape Ferguson* for field support, and to S. Boyle for laboratory assistance. Temperature, salinity, light, and wind data were sourced from the Integrated Marine Observing System (IMOS). IMOS is supported by the Australian Government through the National Collaborative Research Infrastructure Strategy and the Super Science Initiative. This project was funded by an Australian Research Council (ARC) Super Science Fellowship awarded to R. Albright.

Edited by: J.-P. Gattuso

References

- Anthony, K. R. N., Kline, D. I., Diaz-Pulido, G., Dove, S., and Hoegh-Guldberg, O.: Ocean acidification causes bleaching and productivity loss in coral reef builders, *P. Natl. Acad. Sci. USA*, 105, 17442–17446, 2008.
- Anthony, K., Kleypas, J. A., and Gattuso, J.-P.: Coral reefs modify their seawater carbon chemistry – implications for impacts of ocean acidification, *Glob. Change Biol.*, 17, 3655–3666, 2011.
- Bates, N. R., Amat, A., and Andersson, A. J.: Feedbacks and responses of coral calcification on the Bermuda reef system to seasonal changes in biological processes and ocean acidification, *Biogeosciences*, 7, 2509–2530, doi:10.5194/bg-7-2509-2010, 2010.
- Barnes, D. J.: Profiling coral reef productivity and calcification using pH and oxygen electrodes, *J. Exp. Mar. Biol. Ecol.*, 66, 149–161, 1983.
- Barnes, D. J.: Seasonality in community productivity and calcification at Davies reef, Central Great Barrier Reef, *Proceedings of the 6th International Coral Reef Symposium, Australia*, 2, 521–527, 1988.
- Broecker, W. S., Takahashi, T., Simpson, H. J., and Peng, T. H.: Fate of fossil fuel carbon dioxide and the global carbon budget, *Science*, 206, 409–418, 1979.
- Caldeira, K. and Wickett, M. F.: Anthropogenic carbon and ocean pH, *Nature*, 425, p. 365, 2003.
- Canadell, J. G., La Quere, C., Raupach, M. R., Field, C. B., Buitenhuis, E. T., Ciais, P., Conway, T. J., Gillett, N. P., Houghton, R. A., and Marland, G.: Contributions to accelerating atmospheric CO₂ growth from economic activity, carbon intensity, and efficiency of natural sinks, *P. Natl. Acad. Sci. USA*, 104, 18866–18870, 2007.

- Dickson, A. G.: Thermodynamics of the dissociation of boric acid in synthetic seawater from 273.15 to 318.15 °K, *Deep-Sea Res.*, 37, 755–766, 1990.
- Dickson, A. G. and Millero, F. J.: A comparison of the equilibrium constants for the dissociation of carbonic acid in seawater media, *Deep-Sea Res.*, 34, 1733–1743, 1987.
- Dickson, A. G., Sabine, C. L., and Christian, J. R. (Eds.): Guide to best practices for ocean CO₂ measurements, PICES Special Publication 3, North Pacific Marine Science Organization, 2007.
- Doney, S., Fabry, V., Feely, R., and Kleypas, J.: Ocean acidification: the other CO₂ problem, *Ann. Rev. Mar. Sci.*, 1, 169–192, 2009.
- Falter, J. L., Lowe, R. J., Atkinson, M. J., Monismith, S. G., and Schar, D. W.: Continuous measurements of net production over a shallow reef community using a modified Eulerian approach, *J. Geophys. Res.*, 113, C07035, doi:10.1029/2007JC004663, 2008.
- Falter, J. L., Lowe, R. J., Atkinson, M. J., and Cuet, P.: Seasonal coupling and de-coupling of net calcification rates from coral reef metabolism and carbonate chemistry at Ningaloo Reef, Western Australia, *J. Geophys. Res.*, 117, C05003, doi:10.1029/2011JC007268, 2012.
- Falter, J. L., Lowe, R. J., Zhang, Z., and McCulloch, M.: Physical and biological controls on the carbonate chemistry of coral reef waters: effects of metabolism, wave forcing, sea level, and geomorphology, *PLoS One*, 8, e53303, doi:10.1371/journal.pone.0053303, 2013.
- Feely, R. A., Doney, S. C., and Cooley, S. R.: Ocean acidification: present conditions and future changes in a high-CO₂ world, *Oceanography*, 22, 36–47, 2009.
- Frith, C. A.: Windward reef circulation, Davies Reef, central Great Barrier Reef, in: Proceedings of the Inaugural Great Barrier Reef Conference, edited by: Baker, J. T., Carter, R. M., Sammarco, P. W., and Stark, K. P., James Cook University, Townsville, 435–440, 1983.
- Gattuso, J.-P., Pichon, M., Delesalle, B., Canon, C., and Frankignoulle, M.: Carbon fluxes in coral reefs. I. Lagrangian measurement of community metabolism and resulting air-sea CO₂ disequilibrium, *Mar. Ecol.-Prog. Ser.*, 145, 109–121, 1996.
- Gattuso, J.-P., Allemand, D., and Frankignoulle, M.: Photosynthesis and calcification at cellular, organismal and community levels in coral reefs: a review on interactions and control by carbonate chemistry, *Am. Zool.*, 39, 160–183, 1999.
- Gray, S. E. C., DeGrandpre, M. D., Langdon, C., and Corredor, J. E.: Short-term and seasonal pH, pCO₂ and saturation state variability in a coral-reef ecosystem, *Global Biogeochem. Cy.*, 26, GB3012, doi:10.1029/2011GB004114, 2012.
- Halley, R. B. and Yates, K. K.: Will reef sediments buffer corals from increased global CO₂?, in: Proceedings of the 9th International Coral Reef Symposium, Abstracts: Indonesia, State Ministry for the Environment, 2000.
- Ho, D. T., Law, C. S., Smith, M. J., Schlosser, P., Harvey, M., and Hill, P.: Measurements of air-sea gas exchange at high wind speeds in the Southern Ocean: Implications for global parameterizations, *Geophys. Res. Lett.*, 33, L16611, doi:10.1029/2006GL026817, 2006.
- IMOS 2012: Davies Reef Salinity, <http://www.aims.gov.au/docs/data/data.html>, last access: 16 January 2013.
- IPCC, Climate Change 2007: The Physical Science Basis. Contribution of Working Group I to the Fourth Assessment Report of the Intergovernmental Panel on Climate Change, edited by: Solomon, S., Qin, D., Manning, M., Chen, Z., Marquis, M., Averyt, K. B., Tignor, M., and Miller, H. L., Cambridge University Press, Cambridge, United Kingdom and New York, NY, USA, 996 p., 2007.
- Kinsey, D. W.: Productivity and calcification estimates using slack-water period and field enclosures, in: *Coral Reef Research Methods*, Monogr. Oceanogr. Methodol., 5, edited by: Stoddart D. R. and Johannes, R. E., 439–468, UNESCO, Paris, 1978.
- Kinsey, D. W.: Carbon turnover and accumulation by coral reefs, PhD thesis, 248 pp., University of Hawaii, Honolulu, 1979.
- Kinsey, D. W.: Metabolism, calcification, and carbon production: system level studies, in: Proceedings of the 5th International Coral Reef Congress, Tahiti, 4, 505–526, 1985.
- Kleypas, J. A., Buddemeier, R. W., Archer, D., Gattuso, J.-P., Langdon, C., and Opdyke, B. N.: Increased atmospheric carbon dioxide on coral reefs, *Science*, 284, 118–120, 1999.
- Kleypas, J. A., Anthony, K. R. A., and Gattuso, J.-P.: Coral reefs modify their seawater carbon chemistry – case study from a barrier reef (Moorea, French Polynesia), *Glob. Change Biol.*, 17, 3667–3678, 2011.
- Langdon, C. and Atkinson, M. J.: Effect of elevated pCO₂ on photosynthesis and calcification of corals and interactions with seasonal change in temperature/irradiance and nutrient enrichment, *J. Geophys. Res.*, 110, C09S07, doi:10.1029/2004JC002576, 2005.
- Langdon, C., Takahashi, T., Sweeney, C., Chipman, D., Goddard, J., Marubini, F., Aceves, H., Barnett, H., and Atkinson, M. J.: Effect of calcium carbonate saturation state on the calcification rate of an experimental coral reef, *Global Biogeochem. Cy.*, 14, 639–654, 2000.
- Langdon, C., Gattuso, J.-P., and Andresson, A.: Measurements of calcification and dissolution of benthic organisms and communities, in: *Guide to Best Practices for Ocean Acidification Research and Data Reporting*, edited by: Riebesell, U., Fabry, V. J., Hansson, L., and Gattuso, J.-P., 213–232, Eur. Union, Luxembourg, 2010.
- Lewis, E. and Wallace, D. W. R.: Program developed for CO₂ system calculations, in: Carbon Dioxide Information Analysis Center, Oak Ridge National Laboratory, ORNL/CDIAC-105, US Department of Energy, Oak Ridge, TN, 1998.
- Mehrbach, C., Culbertson, C. H., Hawley, J. E., and Pytkowicz, R. M.: Measurement of the apparent dissociation constants of carbonic acid in seawater at atmospheric pressure, *Limnol. Oceanogr.*, 18, 897–907, 1973.
- Ohde, S. and van Woesik, R.: Carbon dioxide flux and metabolic processes of a coral reef, Okinawa, *Bull. Mar. Sci.*, 65, 559–576, 1999.
- Orr, J. C., Fabry, V. J., Aumont, O., Bopp, L., Doney, S. C., Feely, R. A., Gnanadesikan, A., Gruber, N., Ishida, A., Joos, F., Key, R. M., Lindsay, K., Maier-Reimer, E., Matear, R., Monfray, P., Mouchet, A., Najjar, R. G., Plattner, G. K., Rodgers, K. B., Sabine, C. L., Sarmiento, J. L., Schlitzer, R., Slater, R. D., Totterdell, I. J., Weirig, M. F., Yamanaka, Y., and Yool, A.: Anthropogenic ocean acidification over the twenty-first century and its impacts on calcifying organisms, *Nature* 437, 681–686, 2005.
- Sabine, C. L., Feely, R. A., Gruber, N., Key, R. M., Lee, K., Bullister, J. L., Wanninkhof, R., Wong, C. S., Wallace, D. W. R., Tilbrook, B., Millero, F. J., Peng, T. H., Kozyr, A., Ono, T., and

- Rios, A. F.: The oceanic sink for anthropogenic CO₂, *Science*, 305, 367–371, 2004.
- Sabine, C. L., Feely, R. A., Wanninkhof, R., Takahashi, T., Khattiwala, S., and Park, G.: Global oceans [The Global Ocean Carbon Cycle] in State of the Climate in 2010, *B. Am. Meteorol. Soc.*, 92, S100–S105, 2011.
- Santos, I. R., Cook, P. L. M., Rogers, L., de Weys, J., and Eyre, B. D.: The “salt wedge pump”: convection-driven pore-water exchange as a source of dissolved organic and inorganic carbon and nitrogen to an estuary, *Limnol. Oceanogr.*, 57, 1415–1426, 2012.
- Shamberger, K. E. F., Feely, R. A., Sabine, C. L., Atkinson, M. J., DeCarlo, E. H., Mackenzie, F. T., Drupp, P. S., and Butterfield, D. A.: Calcification and organic production on a Hawaiian coral reef, *Mar. Chem.*, 127, 64–75, doi:10.1016/j.marchem.2011.08.003, 2011.
- Shaw, E. C., McNeil, B. I., and Tilbrook, B.: Impacts of ocean acidification in naturally variable coral reef flat ecosystems, *J. Geophys. Res.*, 117, C03038, doi:10.1029/2011JC007655, 2012.
- Silverman, J., Lazar, B., and Erez, J.: Effect of aragonite saturation, temperature, and nutrients on the community calcification rate of a coral reef. *J. Geophys. Res.*, 112, C05004, doi:10.1029/2006jc003770, 2007.
- Silverman, J., Kline, D. I., Johnson, L., Rivlin, T., Schneider, K., Erez, J., Lazar, B., and Caldeira, K.: Carbon turnover rates in the One Tree Island reef: A 40-year perspective, *J. Geophys. Res.*, 117, G03023, doi:10.1029/2012JG001974, 2012.
- Tribollet, A., Godinot, C., Atkinson, M., and Langdon, C.: Effects of elevated pCO₂ on dissolution of coral carbonates by microbial euendoliths, *Glob. Biogeochem. Cy.*, 23, GB3008, doi:10.1029/2008GB003286, 2009.
- Yates, K. K. and Halley, R. B.: CO₃²⁻ concentration and pCO₂ thresholds for calcification and dissolution on the Molokai reef flat, Hawaii, *Biogeosciences*, 3, 357–369, doi:10.5194/bg-3-357-2006, 2006.
- Zeebe, R. E.: History of seawater carbonate chemistry, atmospheric CO₂, and ocean acidification, *Annu. Rev. Earth Pl. Sc.*, 40, 141–165, 2012.